MOLECULAR METABOLISM

Disruption of adipocyte YAP improves glucose homeostasis in mice and decreases adipose tissue fibrosis

Daniel J. Han [1,2], Rukhsana Aslam [2], Paraish S. Misra [1,2], Felix Chiu [2], Tanvi Ojha [2], Apu Chowdhury [4], Carmen K. Chan [1,2], Hoon-Ki Sung [3], Darren A. Yuen [1,2], Cynthia T. Luk [1,2,5,*]

ABSTRACT

Objective: Adipose tissue is a very dynamic metabolic organ that plays an essential role in regulating whole-body glucose homeostasis. Dysfunctional adipose tissue hypertrophy with obesity is associated with fibrosis and type 2 diabetes. Yes-associated protein 1 (YAP) is a transcription cofactor important in the Hippo signaling pathway. However, the role of YAP in adipose tissue and glucose homeostasis is unknown.
Methods: To study the role of YAP with metabolic stress, we assessed how increased weight and insulin resistance impact YAP in humans and mouse models. To further investigate the in vivo role of YAP specifically in adipose tissue and glucose homeostasis, we developed adipose tissue-specific YAP knockout mice and placed them on either chow or high fat diet (HFD) for 12—14 weeks. To further study the direct role of YAP in adipocytes we used 3T3-L1 cells.
Results: We found that YAP protein levels increase in adipose tissue from humans with type 2 diabetes and mouse models of diet-induced obesity and insulin resistance. This suggests that YAP signaling may contribute to adipocyte dysfunction and insulin resistance under metabolic stress conditions. On an HFD, adipose tissue YAP knockout mice had improved glucose tolerance compared to littermate controls. Perigonadal fat pad weight was also decreased in knockout animals, with smaller adipocyte size. Adipose tissue fibrosis and gene expression associated with fibrosis was decreased in vivo and in vitro in 3T3-L1 cells treated with a YAP inhibitor or siRNA.
Conclusions: We show that YAP is increased in adipose tissue with weight gain and insulin resistance. Disruption of YAP in adipocytes prevents glucose intolerance and adipose tissue fibrosis, suggesting that YAP plays an important role in regulating adipose tissue and glucose homeostasis with metabolic stress.

1. INTRODUCTION

Adipose tissue is increasingly recognized as a dynamic metabolic organ capable of rapid remodeling to regulate nutrient excess or shortage [1]. It takes as little as one week of a high fat diet (HFD) in rodents for adipocytes to undergo massive expansion [2]. The weight of visceral adipose tissue can double with one week of HFD and then undergo a dramatic reduction with 24 h of fasting [3]. This plasticity contributes to the essential role of adipose tissue in maintaining metabolic homeostasis.

Increasingly, obesity with adipose tissue fibrosis has been associated with insulin resistance, potentially via reduced plasticity and increased lipotoxicity [4—6]. Increased extracellular matrix (ECM) components, collagen expression and fibrosis in human adipose tissue have been correlated with insulin resistance and higher triglyceride levels [4,5,7]. The mechanisms regulating adipose tissue fibrosis and glucose homeostasis are a rapidly evolving area of interest.

Yes-associated protein 1 (YAP) was first identified as a proline-rich phosphoprotein that binds to the Src homology domain 3 of the Yes proto-oncogene product [8]. Since then, it has been extensively studied in relation to its role in organ size, stem cell fate, and cancer [9—11].

Emerging evidence suggests an important role for Hippo signaling in fibrosis. YAP/TAZ have been identified as mechanosensors that play

[1]Institute of Medical Science, University of Toronto, Toronto, ON, Canada [2]Keenan Centre for Biomedical Science, St. Michael's Hospital, Unity Health Toronto, Toronto, ON, Canada [3]The Hospital for Sick Children Research Institute, Toronto, Ontario, Canada [4]Faculty of Materials and Chemical Engineering, Yibin University, Yibin, Sichuan 644000, China [5]Division of Endocrinology and Metabolism, Department of Medicine, St. Michael's Hospital, Unity Health Toronto, ON, Canada

*Corresponding author. Li Ka Shing Knowledge Institute, St. Michael's Hospital, 209 Victoria Street, 5th Floor, Toronto Ontario M5B 1T8, Canada. E-mail: c.luk@mail.utoronto.ca (C.T. Luk).

Original Article

Table 1 — Primers sequences used for QPCR.

Gene	Forward (5' — 3')	Reverse (5' — 3')
Acta2	CTGACAGAGGCACCACTGAA	CATCTCCAGAGTCCAGCACA
b-actin	AGATGTGGATCAGCAAGCAG	GCGCAAGTTAGGTTTTGTCA
Cidea	TGACATTCATGGGATTGCAGAC	GGCCAGTTGTGATGACTAAGAC
Col1a1	AAGAGGCGAGAGAGGTTTCC	AGAACCATCAGCACCTTTGG
Col3a1	CTGTAACATGGAAACTGGGGAAA	CCATAGCTGAACTGAAAACCACC
Col4a1	TTCTCCCTTTTGTCCCTTCAC	GCTTCTGCTGCTCTTCGC
Col6a1	CTGCTGCTACAAGCCTGCT	CCCCATAAGGTTTCAGCCTCA
F4/80	CTTTGGCTATGGGCTTCCAGTC	GCAAGGAGGACAGAGTTTATCGTG
Gapdh	AGGTCGGTGTGAACGGATTTG	TGTAGACCATGTAGTTGAGGTCA
Hprt	TCAGTCAACGGGGGACATAAA	GGGGCTGTACTGCTTAACCAG
Il1b	AAATACCTGTGGCCTTGGGC	CTTGGGATCCACACTCTCCAG
Il6	CTCTGGGAAATCGTGGAAATG	AAGTGCATCATCGTTGTTCATACA
Il10	AAGGCAGTGGAGCAGGTGAA	CCAGCAGACTCAATACACAC
iNOS	GAGGCCCAGGAGGAGAGAGATCCG	TCCATGCAGACAACCTTGGTGTTG
Lox	CAGCCACATAGATCGCATGGT	GCCGTATCCAGGTCGGTTC
Mcp1	CCACTCACCTGCTGCTACTCA	TGGTGATCCTCTTGTAGCTCTCC
Mmp3	ACATGGAGACTTTGTCCCTTTTG	TTGGCTGAGTGGTAGAGTCCC
Mmp9	GCGTCGTGATCCCCACTTAC	CAGGCCGAATAGGAGCGTC
Mmp13	TGCTTCCTGATGATGACGTTCAAGG	TGGGATGCTTAGGGTTGGGGTC
Pgc1a	CCAGCCTCTTTGCCCAGATC	CGCTACACCACTTCAATCCACC
Ppara	TCAGGGTACCACTACGGAGT	CTTGGCATTCTTCCAAAGCG
Prdm16	CCACCAGCGAGGACTTCAC	GGAGGACTCTCGTAGCTCGAA
Taz	GCGTGCCCAGAAAGATGAA	AGGATCTTTTTCCGGCCACGA
Tgfb	ACCATGCCAACTTCTGTCTGGGAC	ACAACTGCTCCACCTTGGGCTTG
Tnfa	CTGTGAAGGGAATGGGTGTT	TTGGACCCTGAGCCATAATC
Tmem26	GCACCATCACTAGAGACCAAC	ACAAGAATGCCAGAGACCAG
Ucp1	GTGAAGGTCAGAATGCAAGC	AGGGCCCCCTTCATGAGGTC
Yap	AAGACACTGCATTCTGAGTCC	GAATATCAATCCCAGCACAGC

an important role in renal fibrogenesis; knocking out or pharmacological inhibition of YAP reduces renal fibrosis [12]. Lungs of patients with idiopathic pulmonary fibrosis show induced YAP and knocking down YAP reversed these profibrotic changes [13]. In liver fibrosis, YAP is activated in hepatic stellate cells in response to liver damage in vivo and ECM stiffening ex vivo. Importantly, knockdown of YAP expression and pharmacological inhibition of YAP both prevented hepatic stellate cell activation and impeded fibrogenesis in mice [14]. Studies to date of the Hippo signaling pathway and its downstream effectors in adipocytes have focused on adipogenesis, suggesting that in vitro, this pathway may regulate differentiation and proliferation in adipocytes [15,16]. In mature adipocytes in vivo, TAZ has been identified as a regulator of adipogenic activity, with deletion of TAZ in adipocytes resulting in improved glucose homeostasis [17]. Deletion of both YAP and TAZ impairs adipose tissue expansion in mice [18]. The specific role of YAP in mature adipocytes and in whole body glucose homeostasis is not known, and our goal is to characterize its role in adipose tissue, particularly in vivo and in the setting of obesity and type 2 diabetes.

In this study, we find that levels of YAP are increased in adipocytes from humans and mouse models with obesity and insulin resistance. To specifically study the role of YAP in whole body physiology and metabolic stress we generated novel adipocyte-specific YAP knockout mice. Deletion of YAP in fat cells improves glucose tolerance, particularly in the setting of diet-induced obesity and insulin resistance. Targeting YAP also resulted in decreased perigonadal fat pad weight, adipocyte size, and adipose tissue fibrosis. Inhibiting or knocking down YAP in 3T3-L1 adipocytes directly also decreases fibrotic gene expression. Overall, this identifies an important new role for adipocyte YAP in regulating adiposity, glucose homeostasis, and adipose tissue fibrosis in the setting of obesity-associated insulin resistance.

2. METHODS

2.1. Animals

Adiponectin-Cre^+ mice (Jackson Laboratory, Bar Harbor, ME, USA) were crossed with *YAP flox* mice generated from *Taz flox/Yap flox* mice, a gift from Jeff Wrana (Mount Sinai Hospital, Toronto, ON, Canada), to generate $AdipoqCre^+ YAP^{+/-}$ mice [19,20]. These mice were then intercrossed to generate mice with adipocyte-specific deletion of YAP ($AdipoqYAP^{-/-}$) and maintained on a C57Bl/6 background [21,22]. Littermate $AdipoqYAP^{+/+}$ mice were used as controls. Genotypes were confirmed by PCR using DNA from an ear notch.

Prior to weaning, ear clips were obtained from 12 to 14-day old pups and digested using the REDExtract-N-Amp Tissue™ PCR Kit (Sigma—Aldrich, St. Louis, MO, USA). All primers used for mouse genotyping were purchased from Integrative DNA Technologies, Skokie, IL, USA. For *Cre* genotyping, the forward 5'-GGC AGT AAA AAC TAT CCA GCA A-3' and reverse 5'-GTT ATA AGC AAT CCC CAG AAA TG-3' primers were used. For *YAP* genotyping, the forward 5'-AAG ACA CTG CAT TCT GAG TCC-3' and reverse 5'-GAA TAT CAA TCC CAG CAC AGC-3' primers were used. The following program was used for the PCR: the melting temperature was 94 °C for 4 min, the annealing temperature was 60 °C for 30 s, and the primer extension phase was 72 °C for 30 s for 35 cycles. The final PCR product is 204 bp for the wild type allele and 287 bp for the mutant allele.

Mice were housed in a pathogen-free animal facility with a 12-hour light—dark cycle and fed with standard irradiated chow diet ad libitum (5% fat; Harlan Teklad). Starting at 6 weeks of age, mice were randomly assigned to be fed with either HFD (60% fat, 24% carbohydrates, and 16% protein based on caloric content; F3282; Bio-Serv, Flemington, NJ, USA) or standard chow diet for 12 weeks. Animals were excluded from the study if injured or sick, which occurred with similar rates in both knockout and control animals (<1%). Male mice were used where not otherwise specified. All experimental procedures were approved by the Keenan Research Centre for Biomedical Science and Li Ka Shing Knowledge Institute Animal Care Committee.

2.2. *In vivo* metabolic studies

Glucose tolerance tests were performed after fasting the mice overnight (12—16 h), injecting 1 g of glucose per kg of body weight intraperitoneally. Insulin tolerance tests were performed after fasting the mice for 4 h, injecting insulin lispro (Eli Lilly, Indianapolis, IN, USA) 1.0 U per kg of body weight intraperitoneally. Blood glucose measurements were taken at 0, 15, 30, 45, 60, and 120 min after injection using a Contour glucometer (Ascensia Diabetes Care, Parsippany, NJ, USA) [23]. For energy expenditure measurements, mice were individually housed in metabolic cages with free access to water and food. After 24-hour acclimatization period, data for 24 h were collected and analyzed using the Comprehensive Lab Animal Monitoring System (Columbus Instruments, Columbus, OH, USA).

2.3. Adipocyte isolation

Mouse fat pads were removed and thoroughly minced using a razor blade. Minced cells were added to 1 mg/mL of Type I collagenase (Worthington Biochemical, Lakewood, NJ, USA) solution prepared in KRBH buffer. The solution was then incubated at 37 °C and vortexed every 5 min. Cell suspension was centrifuged at 2200 rpm for 10 min and the adipocyte fraction was collected from the supernatant [21]. Total protein extract from cultured human adipocytes was obtained

from Zen-Bio (Durham, NC, USA). Samples were from healthy women with or without diabetes (n = 3; average BMI 39.5; range 26.1—52.1; average age 38; range 37—40 for people without diabetes and n = 3; average BM1 46.8; range 39.5—57.4; average age 43; range 40—47 for people with type 2 diabetes). Subjects with or without obesity and type 2 diabetes who were scheduled for a laparoscopic gastric banding surgical procedure were recruited to provide adipose tissue. Consent was obtained and procedures conducted in accordance with protocols approved by the University and Medical Center Institutional Review Board, East Carolina University, Greenville, NC, USA.

2.4. Cell culture

3T3-L1 preadipocytes were cultured and differentiated as per manu-facturer protocol (ZenBio, Durham, NC, USA). Cells were maintained at 37 °C with 5% CO2 and the media was changed every 2—3 days.

For YAP inhibition, 3T3-L1 mature adipocytes were treated with the drug verteporfin (VP; Tocris Bioscience, Bristol, UK). After 10 days of differentiation, cells were treated with 1.25 μM of VP diluted in dimethyl sulfoxide (DMSO). After a 24-hrs treatment period, cells were washed with sterile 10% phosphate buffered saline (PBS; pH 7.4) and lysates were collected for subsequent analyses.

For TGFβ stimulation, 3T3-L1 mature adipocytes were treated with a recombinant TGFβ1 (Bon Opus Biosciences, Millburn, NJ, USA). After 10 days of differentiation, 10 ng/mL of TGFβ1 was added to cells for 24 h. Cells were washed and lysates were collected following incu-bation for subsequent analyses. To inhibit YAP and stimulate TGFβ signaling simultaneously, 3T3-L1 mature adipocytes were treated with both VP and recombinant TGFβ1 for 24 h.

For YAP knockdown, 3T3-L1 preadipocytes were grown to 70% confluence then treated with Silencer Select Negative Control siRNA (4390843, Ambion) or Silencer Select siRNA for YAP (s20366, Ambion) with Lipofectamine RNAiMAX Transfection Reagent (13778100, Thermo Fisher Scientific) according to the manufacturer's protocol. After 7 days of differentiation, for TGFβ stimulation, 10 ng/mL of TGFβ1 was added to specified adipocytes for 24 h. Cells were washed with PBS and lysates were collected for analyses.

2.5. Immunoblotting

Protein lysates were obtained for Western blots by first crushing the tissues in liquid nitrogen. Cold lysis buffer consisting of RIPA buffer and a protease inhibitor cocktail (sc-24948A; Santa Cruz Biotechnology, Dallas, TX, USA) was then added to the crushed tissues to mechani-cally homogenize using the ultrasonic processors (Betatek, Toronto, ON, Canada). Protein concentrations were then measured using the Bradford protein assay (Sigma—Aldrich, St. Louis, MO, USA) with a microplate spectrophotometer (Molecular Devices, Sunnyvale, CA, USA). After determination of the protein concentrations, 30 μg of total protein was combined with Laemmli sample buffer (Bio-Rad Labora-tories, CA, USA) and boiled for 5 min at 95 °C for loading. Protein samples were then run on a 10% sodium dodecyl sulfate-polyacrylamide gel electrophoresis (SDS-PAGE) in a running buffer solution (5 mM Tris base, 192 mM glycine, and 0.1% SDS). Proteins were transferred onto a methanol-hydrated polyvinylidene difluoride (PVDF) membrane. To block non-specific protein binding, membranes were incubated in 5% non-fat dry milk in Tris-buffered saline solution containing 0.1% Tween-20 (TBST, 20 mM Tris-Cl, 136 mM NaCl, and 0.1% Tween-20) for 1 h at room temperature. Membranes were then washed three times with TBST for 15 min. Membranes were incubated overnight at 4 °C with primary antibodies [YAP (1:1000 dilution; sc-101199; Santa Cruz Biotechnology, Dallas, TX, USA), phospho-YAP (p-YAP) (1:1000 dilution; D9W2I; Cell Signaling Technology, Danvers,

MA, USA), glyceraldehyde-3-phosphate dehydrogenase (GAPDH) (1:10,000 dilution; 14C10; Cell Signaling Technology, Danvers, MA, USA), and β-actin (1:5000 dilutions; A1978; Sigma—Aldrich)]. After overnight incubation, membranes were washed three times with TBST for 15 min, then incubated in secondary HRP-conjugated polyclonal goat anti-mouse antibody (1:5000 dilution; ab6789) or HRP-conjugated polyclonal goat anti-rabbit antibody (1:5000 dilution; ab6721) in 5% non-fat dry milk diluted in TBST for 1 h at room temperature. All secondary antibodies were purchased from Abcam (Cambridge, UK). Membranes were washed three times with TBST for 15 min. Membranes were then incubated with Amersham™ ECL Prime Western Blotting detection reagent (GE Healthcare UK, Buck-inghamshire, UK) at room temperature to expose the membranes and imaged using ChemiDoc™ Touch Imaging System (Bio-Rad Labora-tories). Protein band intensities were quantified using Fiji software (Schindelin et al., 2012).

2.6. RNA isolation and quantitative real-time PCR

Adipocyte RNA was isolated by following the modified steps from the routine RNeasy Plus Universal Mini Kit protocol (Qiagen, Hilden, Ger-many) [24]. RNA was reverse transcribed by random primers and quantitative reverse transcription PCR was performed with SYBR Green master mix reagent (Applied Biosystems, Foster City, CA, USA). Primer sequences are listed in Table 1. Data analysis was performed using the comparative C_t method.

2.7. Histology

Mouse fat pads were isolated and fixed in 4% paraformaldehyde. Sections were then stained with haematoxylin and eosin. Adipocyte size and quantity were measured using Fiji software [25].

For immunofloresence staining, sections were permeabilized with PBST for 20 min then blocked using DAKO Protein Block Serum-Free (Agilent X0909) for an hour. Sections were stained with anti-YAP IgG (Cell Signaling #14074) at 1:100 dilution overnight at 4 °C. Alexa Fluor 647 conjugated anti-rabbit IgG (Thermofisher Catalog # A-21245) at 1:300 dilution was applied for 1 h at room temperature followed by Alexa Fluor 555 conjugated anti-perilipin IgG (Thermofisher Catalog # PA1-1051-A555) at 1:100 dilution for 1 h at room temperature. DAPI (Thermofisher Catalog # 62248) at 1:1000 dilution was then applied for 10 min and sections subsequently mounted with DAKO Fluorescent mounting media (Agilent GM304). Three 5-min washes with PBS were done between each staining step and before mounting. Images were taken with a ZEISS Axio Scan.Z1 Slide Scanner and nuclear localization quantified using ImageJ.

2.8. Human adipocyte transcriptomics data analysis

Pre-normalized (Transcript per Million, TPM) bulk RNA sequencing data of 454 periumbilical subcutaneous adipose tissue biopsies were obtained from Gene Expression Omnibus (GEO) accession GSE135134 [26]. TPM expression values for each were correlated with patient BMI, and correlation Rho coefficients were used in Gene Set Enrichment Analysis (GSEA-Preranked), performed using GSEA software version 4.1.0 (Broad Institute, Cambridge, MA, USA) [27,28].

Raw count bulk RNA sequencing data of superficial subcutaneous adipose tissue biopsies from 6 healthy patients and 6 patients with obesity and type 2 diabetes mellitus were obtained from GEO acces-sion GSE104674 [29]. Values were normalized using DESeq2 [29], and further pre-processed using the natural log of 1 + normalized counts (log1p). Gene set variation analysis (GSVA) was performed on fully normalized data in R version 3.6.3 (R Foundation for Statistical Computing, Vienna, Austria) using GSVA package version 1.34.0 (using
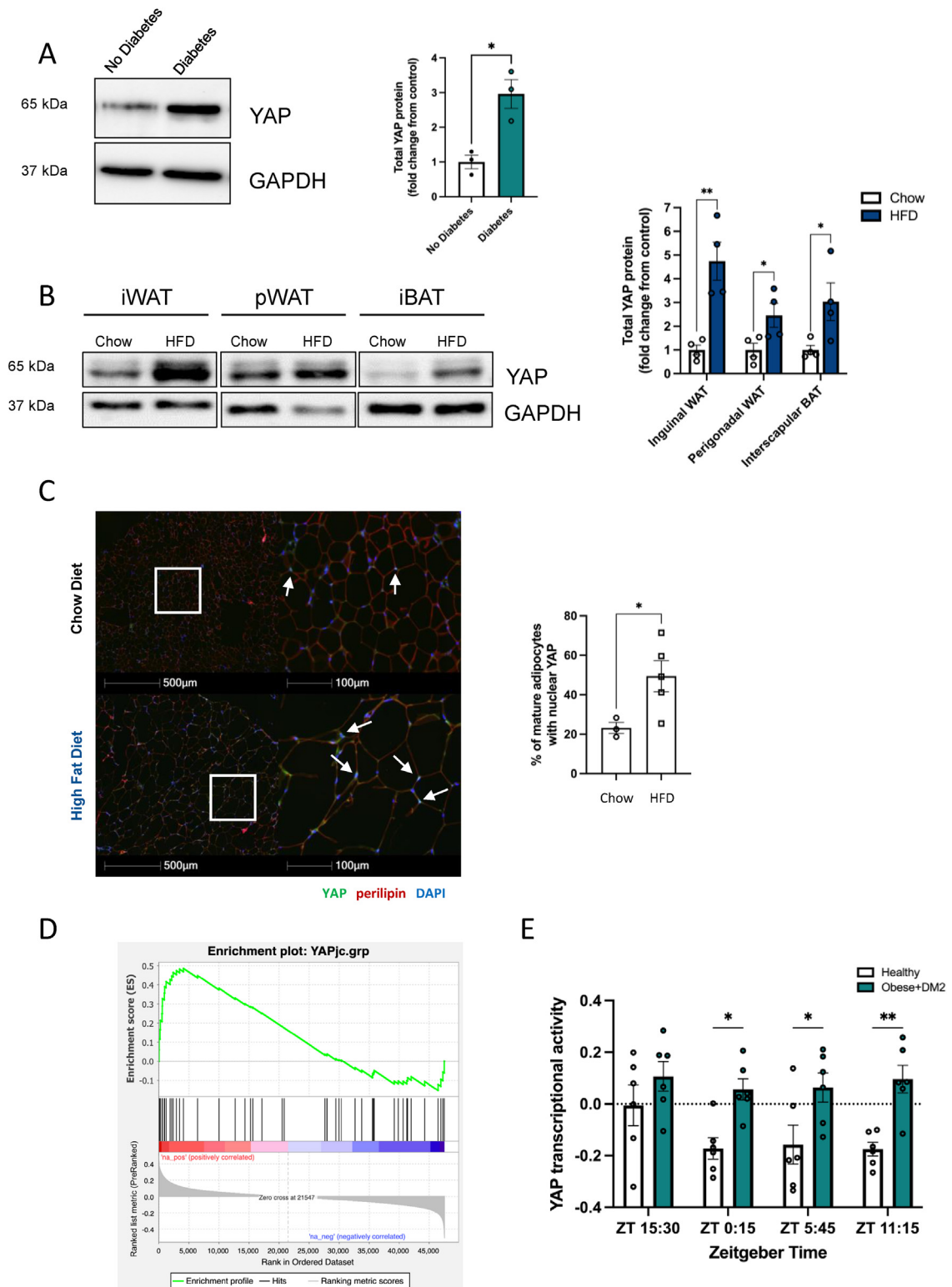
Figure 1: Yap protein is increased in adipose tissue with obesity and insulin resistance. (A) Immunoblot showing YAP protein in omental adipocytes from humans with and without type 2 diabetes (n = 3 per group). Representative sample from a person without and a person with diabetes is shown, with quantification including all samples. (B) Immunoblot of YAP in inguinal, perigonadal, and interscapular brown adipose tissue of mice on high fat diet (HFD) and chow diet, with GAPDH as a loading control (n = 4 per group). Representative samples and quantification of all samples are shown. (C) Immunofluorescence staining and quantification of YAP (green), perilipin (red), and DAPI (blue) in perigonadal adipose tissue of control mice fed with 12 weeks of chow diet and high-fat diet (n = 3−5 per group). Arrows indicate nuclear localization of YAP. (D) Enrichment plot of YAP transcriptional targets among BMI correlated genes. (E) YAP transcriptional activity in healthy and obese individuals with type 2 diabetes at different Zeitgeber Times. iWAT, inguinal white adipose tissue; pWAT, perigonadal white adipose tissue; iBAT, interscapular brown adipose tissue. Data are mean ± SEM. *p < 0.05 and **p < 0.01 by Student's t-test (A, B, C) and two-way ANOVA with Bonferroni's test (E).

 www.molecularmetabolism.com

setting kcdf = "Gaussian") [30], using a recently published Yap transcriptional gene set [31]. GSVA scores were then imported into GraphPad Prism version 9.1.2 (GraphPad Software, San Diego, CA, USA) for further analysis and figure generation.

2.9. Statistics
Data are presented as mean ± standard error of the mean (SEM) and analyzed by two-tailed unpaired Student's t-test for comparisons between two groups, one-way ANOVA with Fischer's LSD test for comparisons between multiple groups, and two-way ANOVA with Bonferroni's post-hoc test for multiple independent variables between multiple groups using GraphPad Prism version 9.1.2 (GraphPad Software, San Diego, CA, USA). Statistical significance was defined as p-value <0.05. *p < 0.05, **p < 0.01, ***p < 0.001, and ****p < 0.0001.

3. RESULTS

3.1. YAP protein is increased in adipose tissue with obesity and insulin resistance
To explore the role of YAP in adipose tissue and glucose homeostasis, we first examined levels of YAP protein in humans and mouse models of insulin resistance. Data from publicly available datasets searchable on BioGPS (http://biogps.org) suggest that white adipose tissue is a significant site of YAP and TAZ expression in both humans and mice. We also found that YAP was robustly present in omental adipocytes from humans, as well as inguinal white adipose tissue (iWAT), perigonadal white adipose tissue (pWAT), and interscapular brown adipose tissue (iBAT) from mice (Figure 1A, B, Supplementary Fig. 1). Furthermore, YAP was increased in omental adipocytes from humans with type 2 diabetes compared to humans without diabetes (Figure 1A). We saw similar results in a mouse model of diet-induced obesity and insulin resistance. YAP protein levels were increased in iWAT, pWAT, and iBAT from mice fed a HFD for 12 weeks (Figure 1B). In this setting, YAP phosphorylation also appeared decreased in iWAT but not consistently different in pWAT (Supplementary Figs. 2A-C). An increase in YAP was more prominent in adipose tissue compared to other glucoregulatory tissues examined, such as liver and muscle (Supplementary Figs. 3A—C). In addition to examining YAP levels, we performed immunofluorescence staining to examine intracellular YAP localization. In the setting of metabolic stress, we saw an increased percentage of adipocytes with nuclear localization of YAP (Figure 1C). We also looked at whether there is an increase in YAP transcriptional signature in adipocytes from patients with diabetes or metabolic syndrome versus healthy individuals. Using publicly available adipocyte transcriptomics data, we reviewed and analyzed for changes in adipocyte YAP transcriptional activity in the setting of obesity, insulin resistance, and diabetes. A study by Raulerson et al. used participants from the METabolic Syndrome in Men (METSIM) study, which is a population-based cohort study of 10,197 males of Finnish ancestry in Finland [26]. A subset of 550 patients from METSIM who underwent periumbilical subcutaneous adipose tissue biopsies were used in the study. A total of 434 patients were included in the final data analysis. BMI data was available for each patient. We performed Gene Set Enrichment Analysis (GSEA), which compares enrichment of a group of genes between groups of samples or patients. This generated a p-value and an enrichment score for each group of patients compared. GSEA demonstrated a significant enrichment of YAP transcriptional targets among BMI-correlated genes in this cohort (p-value <0.001)

(Figure 1D). Another study by Stenvers et al. recruited six obese individuals with type 2 diabetes and six healthy control patients [29]. Superficial subcutaneous adipose tissue samples were obtained by needle aspirations at various individual zeitgeber time (ZT) to study the difference between obese individuals with type 2 diabetes and healthy lean control individuals in the diurnal rhythms of the subcutaneous adipose tissue transcriptome. We found that YAP transcriptional activity was significantly increased in obese individuals with type 2 diabetes compared to healthy control individuals at all four ZTs (Figure 1E). Collectively, these data suggest that YAP protein level, nuclear localization and transcriptional activity increases in adipocytes with metabolic disease, implicating that YAP may play a role in the context of adipose tissue expansion and insulin resistance.

3.2. Generation of adipocyte-specific YAP knockout mice
To further study the role of YAP specifically in adipose tissue and in whole body metabolism, we generated novel adipocyte-specific YAP knockout mice using a Cre-loxP recombination system. We bred adiponectin-Cre mice expressing Cre recombinase specifically in adipocytes to mice with loxP sites flanking exon 2 of the *Yap1* gene to generate *AdipoqYAP*$^{-/-}$ mice (Figure 2A) [19,20]. Genotypes of experimental mice were confirmed by PCR (Figure 2B). Both YAP protein and gene expression were significantly decreased in the major adipose depots of inguinal and perigonadal fat compared to littermate controls, consistent with other reports using adiponectin-Cre systems (Figure 2C,D, Supplementary Fig. 4) [21,22,32,33]. We also measured the expression of TAZ, a YAP paralog, in our knockout model to identify any compensatory changes. There was no difference in the relative expression of *Taz* between *AdipoqYAP*$^{+/+}$ controls and *AdipoqYAP*$^{-/-}$ mice (Figure 2E). Adipocyte-specific YAP knockout mice and littermate *AdipoqYAP*$^{+/+}$ controls appeared healthy and normal. There was no difference in total body weight between knockout and control animals when fed either a chow diet (Figure 2F) or HFD (Figure 2G, Supplementary Fig. 5A).

3.3. Adipocyte-specific disruption of YAP improves glucose tolerance
To identify whether adipocyte YAP plays a role in glucose homeostasis, we measured random and fasting blood glucose levels in chow and HFD-fed *AdipoqYAP*$^{-/-}$ and littermate *AdipoqYAP*$^{+/+}$ control mice. By 12 weeks of age, male *AdipoqYAP*$^{-/-}$ mice on regular chow diet had lower fasting blood glucose levels (Figure 3A). No difference in random blood glucose was seen likely due to greater variability in the fed state (Figure 3B). In the setting of metabolic stress induced by HFD, by 12 weeks of age male *AdipoqYAP*$^{-/-}$ mice had lower fasting blood glucose (Figure 3C) and by 14 weeks of age male *AdipoqYAP*$^{-/-}$ mice also had lower random blood glucose (Figure 3D). With 12 weeks of HFD, female mice did not gain as much weight as male mice, and no difference in fasting blood glucose was seen in this group (Supplementary Figs. 5A and B). On further testing, male HFD-fed *AdipoqYAP*$^{-/-}$ mice had improved glucose tolerance with lower blood glucose levels on glucose tolerance testing (GTT) compared to littermate controls (Figure 3F). No difference was seen at baseline in chow diet-fed mice or in female HFD-fed mice (Figure 3E, Supplementary Fig. 5C). No difference was seen in insulin tolerance testing (ITT) in either males or females (Figure 3G, H, Supplementary Fig. 5D). This suggests that YAP plays an important role in adipocytes and regulation of glucose tolerance, particularly in the setting of diet-induced weight gain.
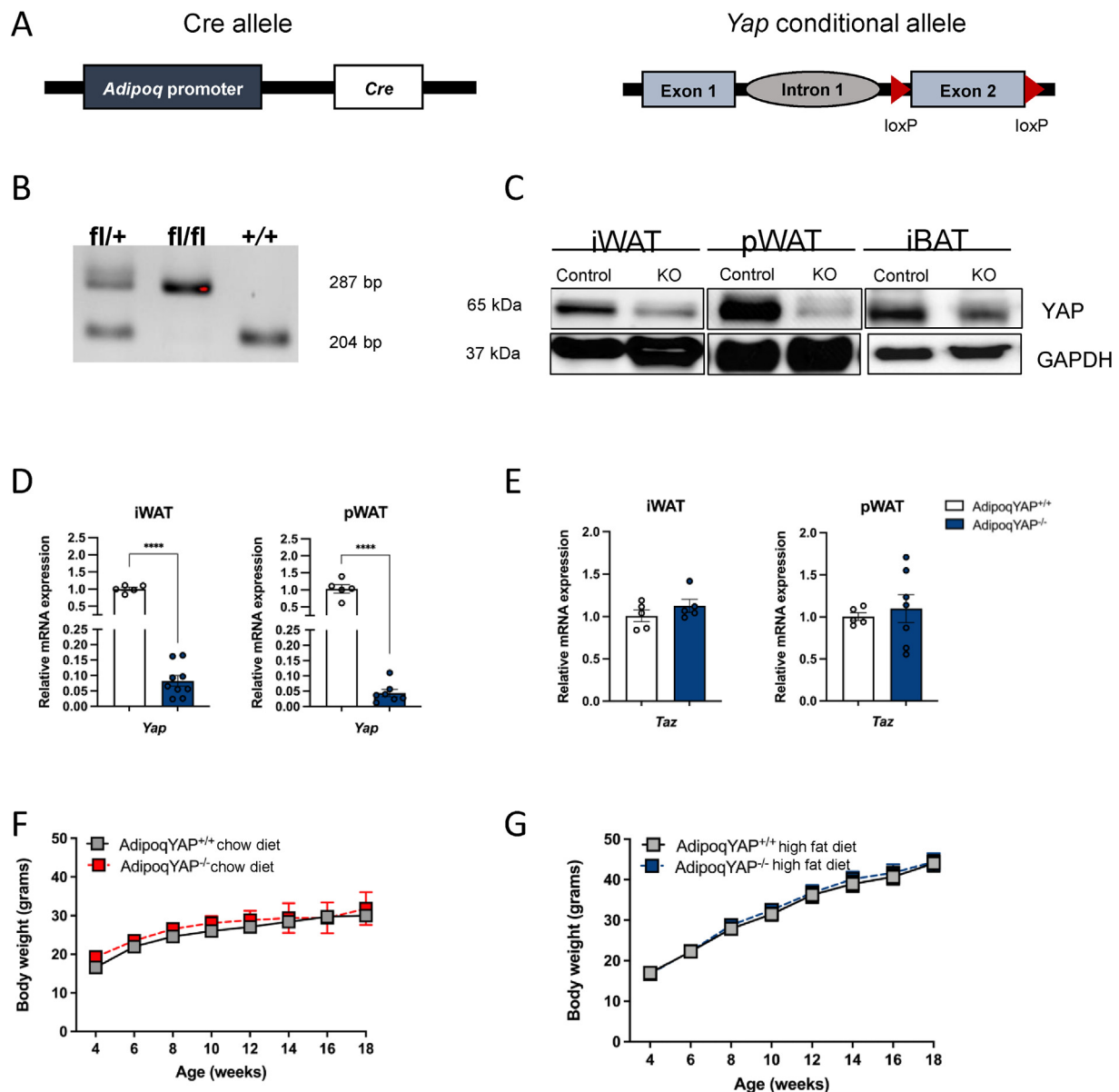
Figure 2: Generation and characterization of adipocyte-specific YAP knockout. (A) Schematic representation of the deleted *Yap1* gene in the adipocyte. (B) PCR genotyping results for YAP heterozygous (fl/+), knockout (fl/fl), and control (+/+) mice. (C) Immunoblot of YAP in iWAT and pWAT, with GAPDH as a loading control. (D,E) Relative expressions of *Yap* (D) and *Taz* (E) mRNA in iWAT and pWAT of AdipoqYAP$^{+/+}$ and AdipoqYAP$^{-/-}$ mice fed with HFD. (F,G) Body weight of AdipoqYAP$^{+/+}$ and AdipoqYAP$^{-/-}$ mice fed with chow diet for 14 weeks (F, n = 3 per group) and HFD for 12 weeks (G, n = 10 per group). iWAT, inguinal white adipose tissue; pWAT, perigonadal white adipose tissue. Data are mean ± SEM. ****p < 0.0001 by Student's *t*-test.

3.4. Knockdown of YAP in adipose tissue decreases perigonadal fat weight in vivo

YAP-mediated signaling can regulate tissue size and dual YAP and TAZ deletion results in decreased adiposity. To determine whether adipocyte YAP alone may regulate adiposity in vivo, we assessed body composition by weighing key fat pads in mice fed chow and HFD. Under basal conditions with chow diet, there was no difference in the perigonadal fat pad weight between *AdipoqYAP*$^{-/-}$ mice and controls (Figure 4A). In the HFD-fed setting, perigonadal fat pad weight was decreased in *AdipoqYAP*$^{-/-}$ mice compared to controls (Figure 4B). Consistent with the lower observed fat pad weight with HFD, we saw smaller adipocytes in perigonadal fat pad as seen on H&E staining, adipocyte size distribution, and average adipocyte diameter (Figure 4C−E). This was associated with a larger number of smaller

adipocytes in knockout mice compared to littermate controls (Figure 4F). No difference in circulating triglyceride or cholesterol levels were seen between groups (Figure 4G). Overall, this demonstrates that YAP regulates fat pad size in vivo via determination of adipocyte size and number in the setting of nutrient excess.

3.5. Deletion of YAP does not alter regulation of whole-body energy homeostasis

Because of the lower adiposity seen in *AdipoqYAP*$^{-/-}$ mice, we then sought to determine whether adipocyte YAP also regulates whole body energy expenditure. We measured metabolic parameters in individually housed *AdipoqYAP*$^{-/-}$ and littermate control mice. There was no significant difference in energy expenditure, as measured by oxygen consumption in mice (Figure 5A). There was no overall difference in
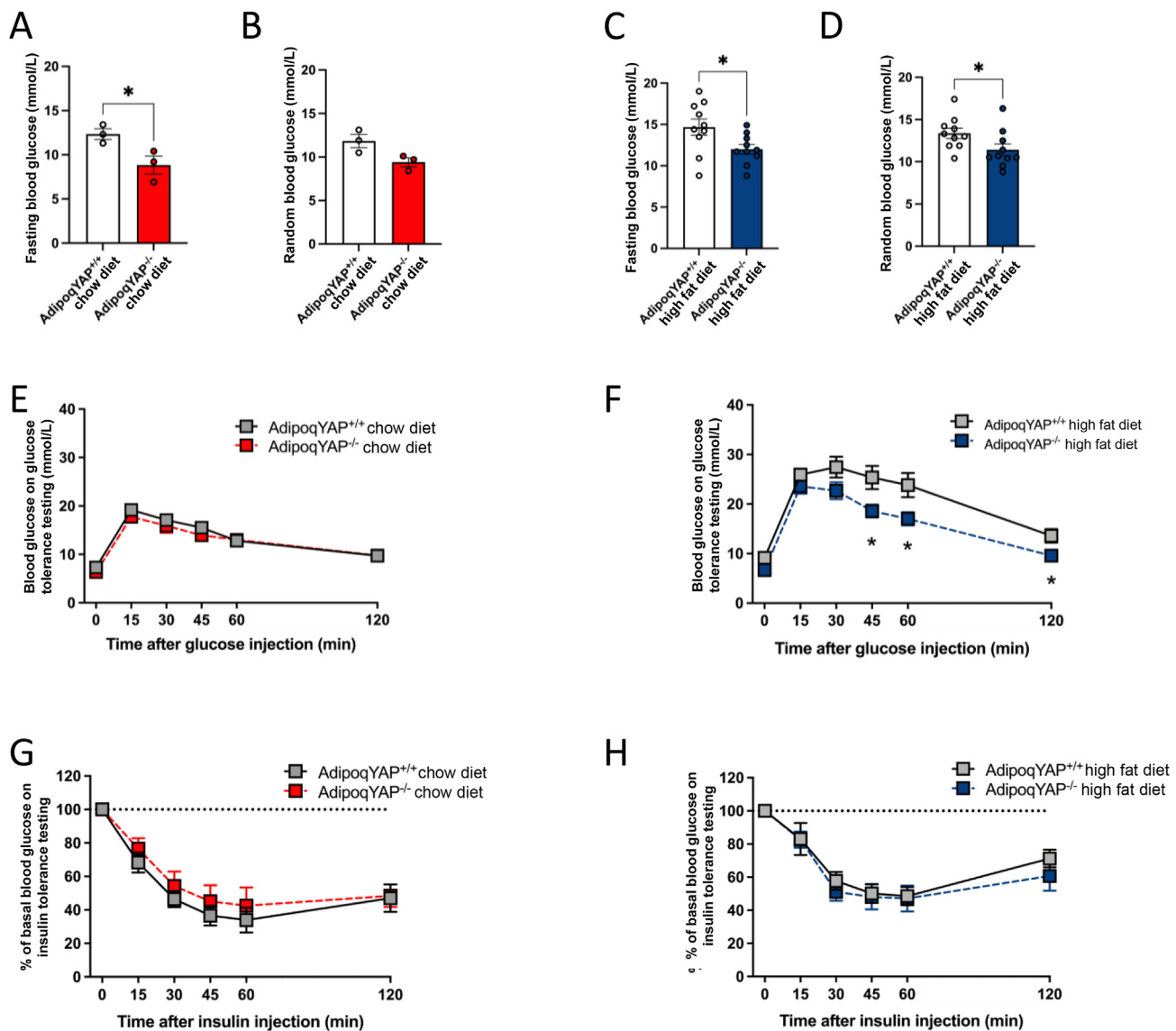
Figure 3: Improved glucose metabolism in adipocyte-specific YAP KO mice. (A,B) Fasting (A) and random (B) blood glucose levels of *AdipoqYAP*^{+/+} and *AdipoqYAP*^{−/−} mice fed with chow diet at 12 weeks of age (n = 3 per group). (C,D) Fasting (C) and random (D) blood glucose levels of *AdipoqYAP*^{+/+} and *AdipoqYAP*^{−/−} mice fed with HFD at 12 weeks—14 weeks of age (n = 10 per group). (E,F) Glucose tolerance test in *AdipoqYAP*^{+/+} and *AdipoqYAP*^{−/−} mice fed with chow diet for 14 weeks (E, n = 8-10 mice per group) and HFD for 12 weeks (F, n = 7-8 mice per group). (G,H) Insulin tolerance test in *AdipoqYAP*^{+/+} and *AdipoqYAP*^{−/−} mice fed with chow diet for 14 weeks (G, n = 8-10 per group) and HFD for 12 weeks (H, 10 mice per group). Data are mean ± SEM. *p < 0.05 by Student's *t*-test.

fuel utilization measured by respiratory exchange ratio (Figure 5B). Body temperature and locomotor activity were also not significantly different (Figure 5C, D). Food intake and water intake were also similar between the two groups (Figure 5E, F). Overall, this suggests a role for YAP in determining adipocyte size and glucose homeostasis that does not significantly alter whole body energy expenditure.

3.6. Adipocyte-specific deletion of YAP decreases inflammation and protects against adipose tissue fibrosis

In the setting of obesity, adipose tissue undergoes pathological remodeling, and this can initiate an inflammatory response, characterized by infiltration of proinflammatory macrophages and increased fibrosis. This increased inflammation and fibrosis in adipose tissue is associated with metabolic complications such as insulin resistance. To see whether adipocyte YAP regulates inflammation in the setting of

nutrient excess, we measured the gene expression of key proinflammatory markers in adipose tissue from *AdipoqYAP*^{−/−} and littermate control mice fed with HFD for 20 weeks. We found that the expression of key proinflammatory cytokines in perigonadal fat from *AdipoqYAP*^{−/−} mice was significantly decreased compared to controls (Figure 6A). This was consistent with lower mRNA expression of *Emr1* and a lower number of crown-like structures (CLSs) as measured by F4/80 immunohistochemical staining in perigonadal fat from *AdipoqYAP*^{−/−} compared to *AdipoqYAP*^{+/+} mice (Figure 6B—D). Emerging data suggest that YAP plays an important role in regulating the development of lung, liver, kidney, and heart fibrosis. However, whether YAP plays a similar role in adipose tissue remains unknown. To gain a better understanding of the role of YAP in the pathophysiology of adipose tissue fibrosis, we measured the expression of key profibrotic genes in *AdipoqYAP*^{−/−} and littermate control mice. Under
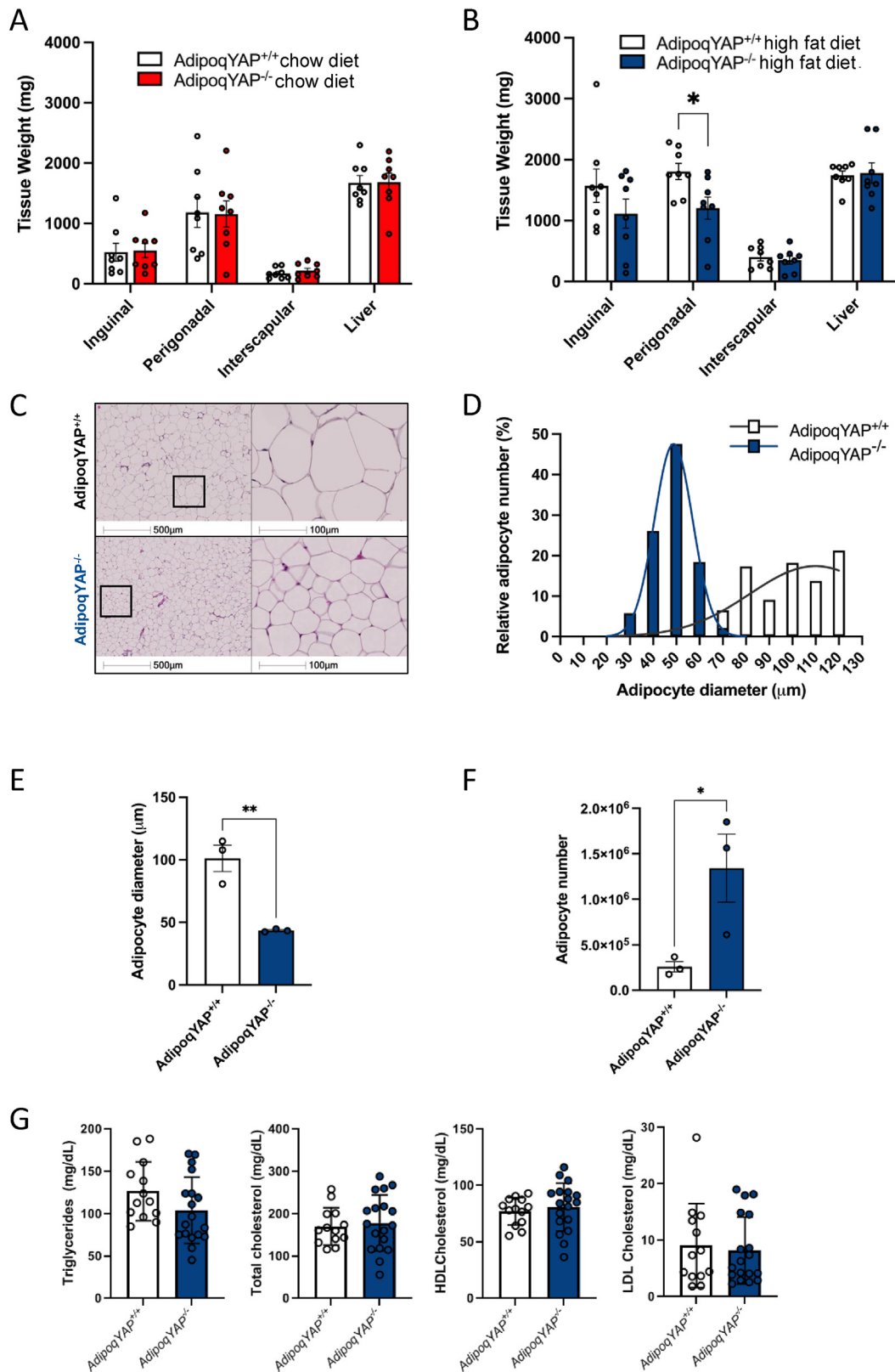
Figure 4: Adiposity is decreased in adipocyte-specific YAP KO mice. (A,B) Weight of tissues at 14 weeks of chow diet (A) and 12 weeks of HFD (B) in *AdipoqYAP*$^{+/+}$ and *AdipoqYAP*$^{-/-}$ mice (n = 8−10 per group). (C) Hematoxylin and eosin staining in perigonadal white adipose tissue from *AdipoqYAP*$^{+/+}$ and *AdipoqYAP*$^{-/-}$ mice fed HFD for 12 weeks. (D) Adipocyte size distribution, (E) average adipocyte diameter, and (F) calculated total adipocyte number in perigonadal white adipose tissue of *AdipoqYAP*$^{+/+}$ and *AdipoqYAP*$^{-/-}$ mice fed with HFD for 12 weeks (n = 3 mice per group). (G) Triglyceride, total cholesterol, HDL cholesterol and LDL cholesterol levels in *AdipoqYAP*$^{+/+}$ and *AdipoqYAP*$^{-/-}$ mice fed HFD for 12 weeks. Data are mean ± SEM. *p < 0.05 and **p < 0.01 by Student's *t*-test.
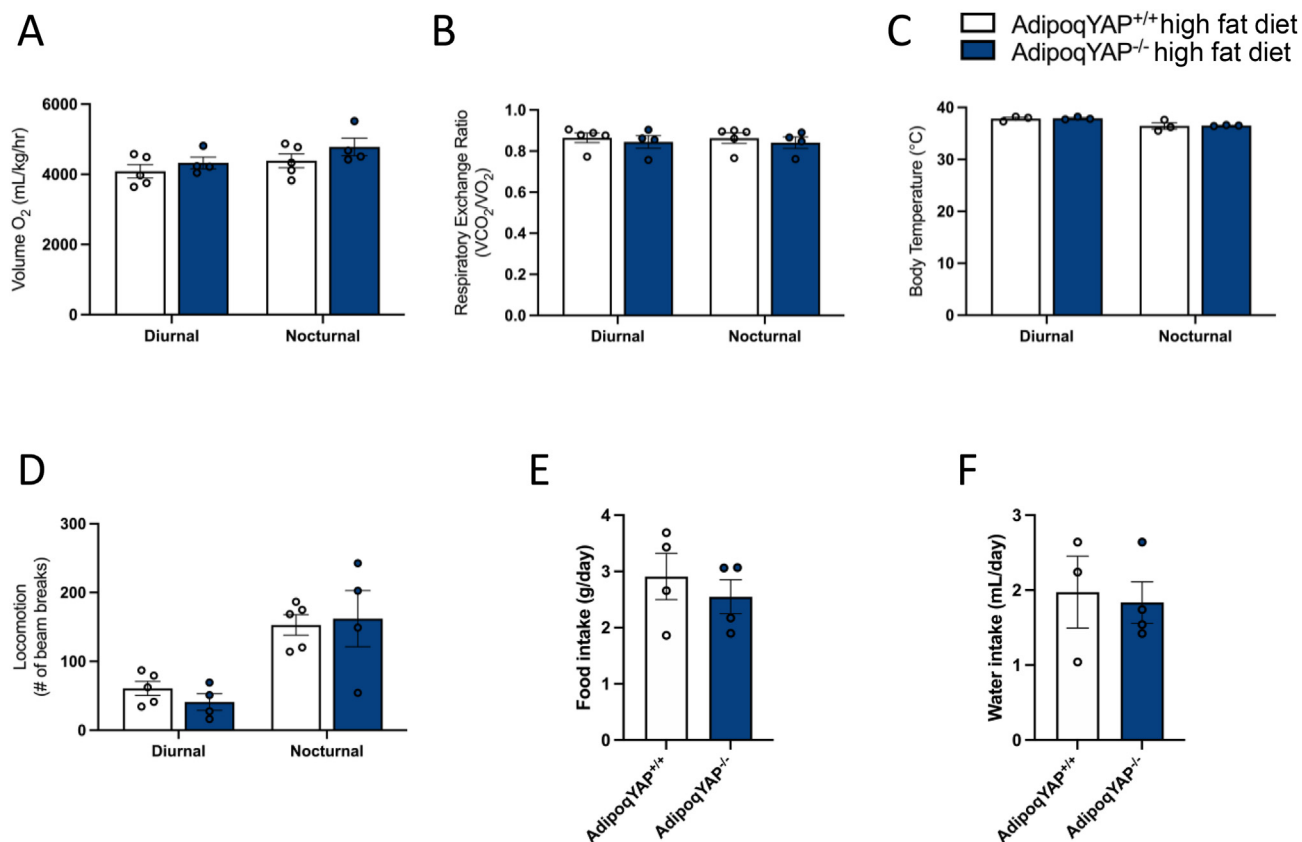
Figure 5: No difference in energy expenditure between adipocyte-specific YAP KO and control mice. (A) Energy expenditure measured by oxygen consumption of *AdipoqYAP*$^{+/+}$ and *AdipoqYAP*$^{-/-}$ mice on 20 weeks of HFD (n = 4−5 mice per group). (B) Fuel utilization measured by respiratory exchange ratio (RER) of *AdipoqYAP*$^{+/+}$ and *AdipoqYAP*$^{-/-}$ mice on 20 weeks of HFD (n = 4−5 mice per group). (C) Body temperature of *AdipoqYAP*$^{+/+}$ and *AdipoqYAP*$^{-/-}$ mice on 20 weeks of HFD (n = 4−5 mice per group). (D) Ambulatory activity of *AdipoqYAP*$^{+/+}$ and *AdipoqYAP*$^{-/-}$ mice on 20 weeks of HFD (n = 4−5 mice per group). (E) Food and (F) water intake of *AdipoqYAP*$^{+/+}$ and *AdipoqYAP*$^{-/-}$ mice on 20 weeks of HFD (n = 3−4 mice per group). Data are mean ± SEM.

HFD-fed setting, we saw a significant reduction in *Col1a1, Col3a1, Col6a1,* and *Tgfb1* in the perigonadal fat from *AdipoqYAP*$^{-/-}$ mice compared to controls (Figure 6E). Furthermore, excess collagen deposition, a characteristic of adipose tissue fibrosis, was seen to a lesser degree as shown by picrosirius red (PSR) staining in perigonadal fat pads from HFD-fed *AdipoqYAP*$^{-/-}$ mice (Figure 6F, G). Overall, this demonstrates that disruption of YAP resulted in decreased inflammation and protected against adipose tissue fibrosis in the setting of metabolic stress induced by HFD.

3.7. Direct inhibition of adipocyte YAP decreases genes involved in fibrosis signaling

Based on our in vivo data and given the central role of YAP in fibrosis, we examined whether YAP directly affects profibrotic gene expression in adipocytes. To address this question, we pharmacologically depleted YAP in differentiated 3T3-L1 adipocytes. Specifically, we administered a drug called verteporfin (VP), which is used to treat patients with macular degeneration. Consistent with previously described inhibitory effects of VP on YAP [12], we found that 3T3-L1 mature adipocytes treated with VP had decreased YAP protein levels compared to cells treated with DMSO (Figure 7A). In addition, targeting YAP using VP led to decreased YAP mRNA levels compared to DMSO-treated controls (Figure 7B). Additionally, we were able to knockdown YAP with siRNA transfection in 3T3-L1 adipocytes, with significantly

decreased YAP protein and mRNA expression levels (Supplementary Figs. 6A and B).

Among the different mediators involved in tissue fibrosis, TGFβ1 is considered a key molecule in the activation of fibrosis signaling. To induce fibrosis in vitro and assess the impact of TGFβ1 on adipocytes, we incubated 3T3-L1 mature adipocytes with recombinant TGFβ1 protein. As previously described, YAP levels were several-fold higher in adipocytes treated with TGFβ1 compared to controls (Figure 7B). We then examined the effect of VP on YAP in the presence of TGFβ1. Simultaneous VP and TGFβ1 treatment decreased YAP gene expression to levels similar to baseline (Figure 7B). Because TAZ is a paralog of YAP, we investigated whether VP exerts a similar inhibitory effect on TAZ in adipocytes. Intriguingly, TAZ expression was not significantly reduced in 3T3-L1 adipocytes treated with VP (Figure 7C). While, TGFβ1 treatment enhanced TAZ expression compared to controls (Figure 7C), we also find that treatment with VP and TGFβ1 did not reduce TAZ levels (Figure 7C).

To assess the impact of VP treatment on fibrosis, qPCR analysis of key profibrotic genes was performed. We first measured TGFβ1 levels in the three treatment groups. As expected, VP treatment significantly reduced *Tgfb1* expression while recombinant TGFβ1 treatment increased *Tgfb1* expression by more than 8-fold compared to cells treated with DMSO (Figure 7D). When VP and TGFβ1 treatment was combined, TGFβ1 expression was only increased by approximately
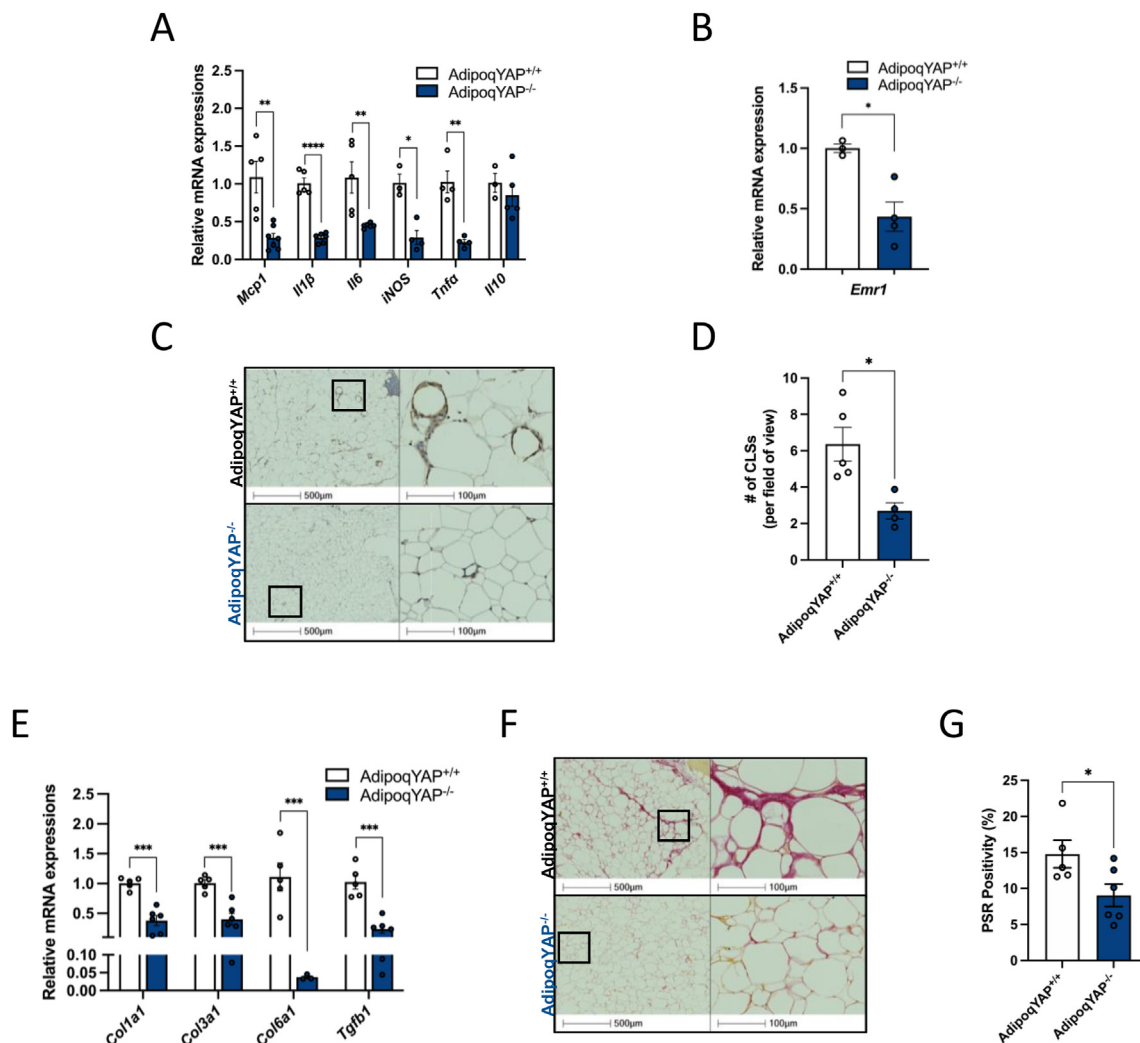
Figure 6: Loss of adipocyte YAP decreases inflammation and protects against adipose tissue fibrosis. (A) Relative mRNA expressions of proinflammatory cytokines in perigonadal white adipose tissue of *AdipoqYAP*$^{+/+}$ and *AdipoqYAP*$^{-/-}$ mice fed with 12 weeks of HFD (n = 3–7 mice per group). (B) Relative expression of *F4/*80 mRNA in perigonadal white adipose tissue of *AdipoqYAP*$^{+/+}$ and *AdipoqYAP*$^{-/-}$ mice on HFD for 12 weeks. (C) Immunohistochemistry staining of F4/80 in perigonadal adipose tissue of *AdipoqYAP*$^{+/+}$ and *AdipoqYAP*$^{-/-}$ mice fed with 12 weeks of HFD. (D) Number of crown-like structures (CLSs) in perigonadal white adipose tissue of *AdipoqYAP*$^{+/+}$ and *AdipoqYAP*$^{-/-}$ mice on HFD for 12 weeks. (E) Relative mRNA expressions of profibrotic genes in perigonadal white adipose tissue in perigonadal white adipose tissue of *AdipoqYAP*$^{+/+}$ and *AdipoqYAP*$^{-/-}$ mice on HFD for 12 weeks. (F) Picrosirius red (PSR) staining and (G) quantification in perigonadal white adipose tissue of *AdipoqYAP*$^{+/+}$ and *AdipoqYAP*$^{-/-}$ mice on HFD for 12 weeks. Data are mean ± SEM. *p < 0.05, **p < 0.01, ***p < 0.001, and ****p < 0.0001 by Student's *t*-test.

1.5-fold (Figure 7D). Next, we measured the expression of key collagens involved in ECM. As shown in Figure 7E—H, collagen expression is significantly reduced with VP treatment. In contrast, these collagen levels are approximately 4-fold higher in the TGFβ1 treatment group compared to controls (Figure 7E—H). However, this increase was no longer present when VP was combined with TGFβ1 (Figure 7E—H).

To further assess the impact of reduced YAP on fibrosis, we measured the expression of additional markers of fibrosis. As expected, VP treatment significantly reduced the mRNA levels of *Acta2* and *Lox*, while TGFβ1 treatment increased their expression, and simultaneous VP and TGFβ1 resulted in a smaller increase (Figure 7I—J). A similar trend in *Lox* expression was seen with siRNA knockdown of YAP (Supplementary Fig. 6C). Next, we measured the expression of MMP-3, -9, and -13, which play an important role in regulating matrix integrity

and stability. Treatment of mature 3T3-L1 adipocytes with VP to inhibit YAP reduced MMP-3, -9, and -13 expressions compared to controls (Figure 7K—M). These MMPs increased two-fold in adipocytes treated with TGFβ1 but not when adipocytes were simultaneously treated with VP (Figure 7K—M). These results suggest that YAP disruption in adipocytes directly reduces expression of fibrosis genes. Overall, this identifies a new role specifically for YAP in adipose tissue inflammation, fibrosis, and glucose metabolism.

4. DISCUSSION

There is a growing need to understand the factors determining adipocyte function in the highly dynamic setting of nutrient excess and metabolic disease. The Hippo signaling pathway is a key player
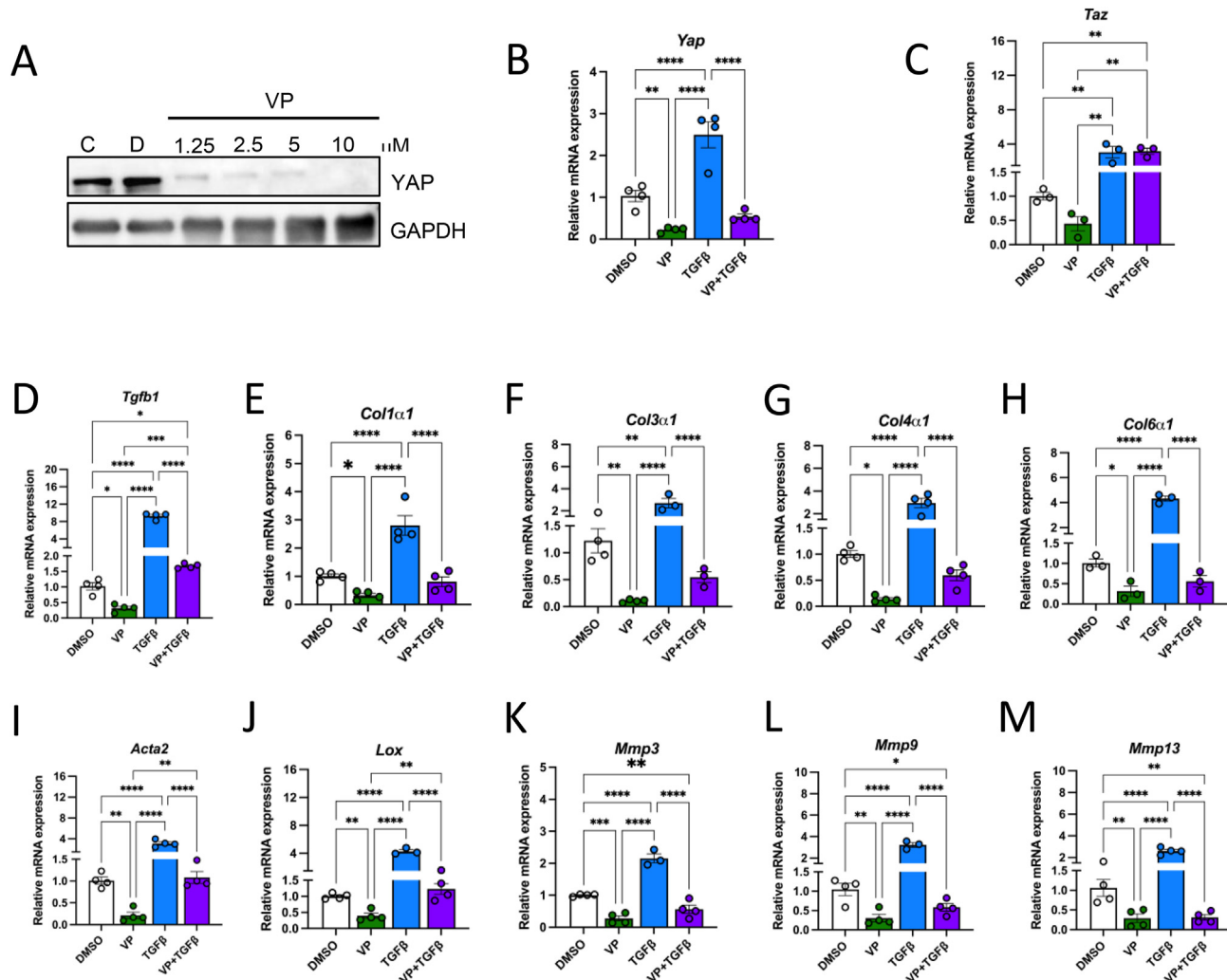
Figure 7: Verteporfin treatment decreases the expression of key profibrotic genes in 3T3-L1 adipocytes. (A) Immunoblot of YAP in differentiated 3T3-L1 adipocytes treated with control (C), DMSO (D), and verteporfin (VP), with GAPDH as a loading control. (B) Relative expressions of *Yap* and (C) *Taz* mRNA in DMSO, VP, TGFb1, and VP + TGFb1 treated cells. (D—M) Relative mRNA expressions of profibrotic genes in DMSO, VP, TGFb1, and VP + TGFb1 treated cells. Data are mean ± SEM. *p < 0.05, **p < 0.01, ***p < 0.001, and ****p < 0.0001 by one-way ANOVA with Fischer's LSD test.

in tissue growth and increasingly recognized for a role in fibrosis. Here, we found that in both humans and mouse models with insulin resistance, YAP is increased in adipocytes. Deletion of adipocyte YAP decreased fasting blood glucose levels and decreased perigonadal fat mass in male mice fed HFD. These findings occurred in the absence of a significant difference in whole body weight, inguinal fat pad weight, interscapular fat pad weight, or energy expenditure. Furthermore, deletion of adipocyte YAP decreased adipose tissue inflammation and fibrosis. These findings suggest that YAP plays an important role in adipocyte determination of whole-body glucose tolerance and protects against HFD-induced inflammation and fibrosis.

A growing number of studies propose a key role for Hippo signaling in adipose tissue. Upon activation, the extracellular signals are transduced to kinases MST1/2, which are associated with tumor suppressor protein Salvador to form an active enzyme complex [10]. This complex phosphorylates and activates large tumor suppressors 1/2 (LATS1/2), which are two kinases that are regulated by Mob1A/1B subunits. Following the activation of LATS1/2, YAP/TAZ are phosphorylated and

inactivated, leading to their accumulation in the cytoplasm and degradation through recruitment of the SCF$^{\beta-TRCP}$ E3 ubiquitin ligase [34—36]. Retention of YAP/TAZ in the cytoplasm inhibits the expression of target genes responsible for cell survival. Conversely, active YAP/TAZ are dephosphorylated and translocated to the nucleus, where it associates with TEA domain (TEAD) family transcription factors to activate the expression of TEAD target genes, including Myc, amphiregulin, Wnts, and connective tissue growth factor (CTGF) [37—39]. Our data suggest that increased YAP levels and YAP nuclear localization in the setting of obesity-associated insulin resistance could contribute to increased activation of gene transcription.

Complementary to our work, previous studies have focused on regulation of adipogenesis, primarily in vitro. TAZ has been implicated in repressing the major adipogenic transcription factor PPARγ in mesenchymal stem cells [16]. Similarly, in 3T3-L1 mature adipocytes, LATS2 was found to phosphorylate YAP and TAZ, decreasing activation of transcription factor TEAD and downstream adipogenic gene transcription [15]. In one model of YAP overexpression, TAZ down-regulation was thought to promote adipogenesis [40]. Finally,

disruption of TAZ in adipocytes was recently shown to increase PPARγ activity to decrease adipose tissue inflammation, improve insulin sensitivity, and glucose tolerance [17]. Collectively, this suggests that adipogenesis via PPARγ activity could potentially be regulated by Hippo signaling. However, further investigation is needed to determine the role of YAP in this context.

Despite these emerging studies on TAZ, the specific role of its paralog YAP is less well known. Studies in vitro in some cell types suggest that similar to TAZ, YAP could regulate adipogenesis. YAP knockdown suppresses differentiation in ovine preadipocytes and rat adipose-derived stem cells [41,42]. Furthermore, a recent study has shown that YAP/TAZ are activated by the proinflammatory cytokines in both human and mouse mature adipocytes to promote adipocyte survival during WAT expansion [18]. Wang et al. further showed that YAP/TAZ regulate the balance between adipocyte death and the formation of new adipocytes in the setting of obesity [18]. However, the specific role of YAP in mature adipocytes and in vivo, particularly with metabolic dysfunction is not known. Our objective was to study the role of YAP in mature adipocytes, in whole body physiology and in the setting of obesity-associated metabolic dysregulation. While others have described that the expression of YAP is less than TAZ in adipose tissue under basal conditions [17], here we found that YAP increases, with increased nuclear localization in adipocytes in the setting of obesity and insulin resistance. Furthermore, we found that YAP transcriptional activity is increased in humans with obesity and type 2 diabetes, suggesting a potentially important role of YAP in gene regulation in the setting of metabolic dysfunction.

The rapid remodeling of adipose tissue is due to the coordinated response of resident adipose tissue cells, including adipocytes, macrophages, endothelial cells, and fibroblasts [43]. With excess nutrient availability, adipocytes increase lipid storage and expand in size. Under normal physiological conditions, adipose tissue mobilizes the surplus of lipids and maintains energy homeostasis during nutrient deprivation [44]. With obesity and insulin resistance, there is increased lipolysis resulting in excess circulating levels of free fatty acids derived from triacylglycerides [45]. This can activate proinflammatory pathways and impair insulin signaling. Consequently, obesity-associated insulin resistance is associated with increased inflammation and macrophage infiltration. We found that $AdipoqYAP^{-/-}$ mice fed with HFD had more and smaller adipocytes. While this could not be accounted for by differences in triglyceride levels, $AdipoqYAP^{-/-}$ mice had less adipose tissue macrophage accumulation and lower expression of proinflammatory and collagen genes compared to littermate controls, consistent with decreased inflammation associated with improved glucose homeostasis.

Adipose tissue inflammation and dysglycemia has been associated with increased fibrosis formation, ultimately leading to metabolically dysfunctional adipose tissue. Several studies have shown that YAP plays an important role in the development of lung, liver, and kidney fibrosis [12—14]. However, the role of YAP in the context of adipose tissue fibrosis is unknown. In the current study, we demonstrated that knocking out YAP in adipocytes reduces the expression of pro-fibrotic genes and decreases collagen deposition in perigonadal white adipose tissue. Our findings suggest that deleting YAP in adipocytes reduces the development of fibrosis in the setting of diet-induced obesity.

Given the important role of YAP in the pathogenesis of fibrosis, we examined whether YAP directly affects adipocytes to regulate fibrosis. To address this question, we inhibited YAP in 3T3-L1 mature adipocytes using a drug called VP and knocked down YAP with siRNA transfection, then measured key profibrotic genes under different settings. Several studies have shown that VP inhibits YAP by disrupting the YAP-TEAD complex [46—48]. Consistent with this finding, we show that 3T3-L1 adipocytes treated with VP decreased YAP protein levels. To induce fibrosis in vitro, we treated differentiated 3T3-L1 adipocytes with recombinant TGFβ1. We show treatment with TGFβ1 led to upregulation of key profibrotic genes in adipocytes. To determine whether pharmacological or genetic inhibition of YAP could reverse TGFβ1-induced fibrosis, we treated the cells with VP or siRNA and TGFβ1 simultaneously. Key profibrotic genes, such as *Lox*, were reduced upon treatment with both VP or siRNA and TGFβ1. This data confirms a direct role of YAP in regulating fibrotic gene expression in adipocytes.

Limitations of this study include its focus on fibrosis. Adipocytes are capable of multiple homeostatic roles, and YAP may have diverse, context-specific functions. Further work is needed to determine if YAP plays a role in adipogenesis in vivo and glucoregulatory gene expression. Also, more work is needed to determine whether acute inhibition of knockdown of YAP in vivo may inhibit fibrosis and ultimately improve glucose homeostasis.

Overall, this study identifies a key novel role for YAP in adipocytes, particularly in the setting of obesity-associated insulin resistance. YAP protein increases in adipose tissue in this setting and deletion of YAP results in decreased adiposity and improved glucose tolerance with diet-induced obesity, potentially via decreases in adipose tissue inflammation and fibrosis. This study improves our understanding of adipose tissue regulation in a model of type 2 diabetes.

AUTHOR CONTRIBUTIONS

DJH, HS, DAY and CTL designed and oversaw the study. DJH, RA, TO, PSM, FC, and CKC conducted experiments and analyzed data. DJH, CTL and AC drafted and revised the manuscript. All authors have reviewed the manuscript.

FINANCIAL SUPPORT

CONFLICT OF INTEREST

None declared.

DATA AVAILABILITY

Data will be made available on request.

APPENDIX A. SUPPLEMENTARY DATA

Supplementary data to this article can be found online at https://doi.org/10.1016/j.molmet.2022.101594.

REFERENCES

[1] Kusminski, C.M., Bickel, P.E., Scherer, P.E., 2016. Targeting adipose tissue in the treatment of obesity-associated diabetes. Nature Reviews Drug Discovery, 639–660. https://doi.org/10.1038/nrd.2016.75.

[2] Li, J., Yu, X., Pan, W., Unger, R.H., 2002. Gene expression profile of rat adipose tissue at the onset of high-fat-diet obesity. American Journal of Physiology - Endocrinology And Metabolism 282(6):45–46. https://doi.org/10.1152/ajpendo.00516.2001.

[3] Kleemann, R., Van Erk, M., Verschuren, L., Van Den Hoek, A.M., Koek, M., Wielinga, P.Y., et al., 2010. Time-resolved and tissue-specific systems analysis of the pathogenesis of insulin resistance. PLoS One 5(1). https://doi.org/10.1371/journal.pone.0008817.

[4] Spencer, M., Unal, R., Zhu, B., Rasouli, N., McGehee, R.E., Peterson, C.A., et al., 2011. Adipose tissue extracellular matrix and vascular abnormalities in obesity and insulin resistance. Journal of Clinical Endocrinology and Metabolism 96(12):E1990–E1998. https://doi.org/10.1210/jc.2011-1567.

[5] Sun, K., Tordjman, J., Clément, K., Scherer, P.E., 2013. Fibrosis and adipose tissue dysfunction. Cell Metabolism 18(4):470–477. https://doi.org/10.1016/j.cmet.2013.06.016.

[6] Savage, D.B., Petersen, K.F., Shulman, G.I., 2007. Disordered lipid metabolism and the pathogenesis of insulin resistance. Physiological Reviews, 507–520. https://doi.org/10.1152/physrev.00024.2006.

[7] Pasarica, M., Gowronska-Kozak, B., Burk, D., Remedios, I., Hymel, D., Gimble, J., et al., 2009. Adipose tissue collagen VI in obesity. Journal of Clinical Endocrinology and Metabolism 94(12):5155–5162. https://doi.org/10.1210/jc.2009-0947.

[8] Sudol, M., 1994. Yes-Associated Protein (YAP65) is a proline-rich phosphoprotein that binds to the SH3 domain of the Yes proto-oncogene product. Oncogene 9(8):2145–2152.

[9] Camargo, F.D., Gokhale, S., Johnnidis, J.B., Fu, D., Bell, G.W., Jaenisch, R., et al., 2007. YAP1 increases organ size and expands undifferentiated progenitor cells. Current Biology 17(23):2054–2060. https://doi.org/10.1016/j.cub.2007.10.039.

[10] Huang, J., Wu, S., Barrera, J., Matthews, K., Pan, D., 2005. The Hippo signaling pathway coordinately regulates cell proliferation and apoptosis by inactivating Yorkie, the Drosophila homolog of YAP. Cell 122(3):421–434. https://doi.org/10.1016/j.cell.2005.06.007.

[11] Piccolo, S., Dupont, S., Cordenonsi, M., 2014. The biology of YAP/TAZ: hippo signaling and beyond. Physiological Reviews 94(4):1287–1312. https://doi.org/10.1152/physrev.00005.2014.

[12] Szeto, S.G., Narimatsu, M., Lu, M., He, X., Sidiqi, A.M., Tolosa, M.F., et al., 2016. YAP/TAZ are mechanoregulators of TGF-b-smad signaling and renal fibrogenesis. Journal of the American Society of Nephrology 27(10):3117–3128. https://doi.org/10.1681/ASN.2015050499.

[13] Liu, F., Lagares, D., Choi, K.M., Stopfer, L., Marinković, A., Vrbanac, V., et al., 2015. Mechanosignaling through YAP and TAZ drives fibroblast activation and fibrosis. American Journal of Physiology - Lung Cellular and Molecular Physiology 308(4):L344–L357. https://doi.org/10.1152/ajplung.00300.2014.

[14] Mannaerts, I., Leite, S.B., Verhulst, S., Claerhout, S., Eysackers, N., Thoen, L.F.R., et al., 2015. The Hippo pathway effector YAP controls mouse hepatic stellate cell activation. Journal of Hepatology 63(3):679–688. https://doi.org/10.1016/j.jhep.2015.04.011.

[15] An, Y., Kang, Q., Zhao, Y., Hu, X., Li, N., 2013. Lats2 modulates adipocyte proliferation and differentiation via hippo signaling. PLoS One 8(8):72042. https://doi.org/10.1371/journal.pone.0072042.

[16] Hong, J.H., Hwang, E.S., McManus, M.T., Amsterdam, A., Tian, Y., Kalmukova, R., et al., 2005. TAZ, a transcriptional modulator of mesenchymal stem cell differentiation. Science 309(5737):1074–1078. https://doi.org/10.1126/science.1110955.

[17] El Ouarrat, D., Isaac, R., Lee, Y.S., Oh, D.Y., Wollam, J., Lackey, D., et al., 2020. TAZ is a negative regulator of PPARγ activity in adipocytes and TAZ deletion improves insulin sensitivity and glucose tolerance. Cell Metabolism 31(1):162–173. https://doi.org/10.1016/j.cmet.2019.10.003 e5.

[18] Wang, L., Wang, S.P., Shi, Y., Li, R., Günther, S., Ong, Y.T., et al., 2020. YAP and TAZ protect against white adipocyte cell death during obesity. Nature Communications 11(1). https://doi.org/10.1038/s41467-020-19229-3.

[19] Eguchi, J., Wang, X., Yu, S., Kershaw, E.E., Chiu, P.C., Dushay, J., et al., 2011. Transcriptional control of adipose lipid handling by IRF4. Cell Metabolism 13(3):249–259. https://doi.org/10.1016/j.cmet.2011.02.005.

[20] Reginensi, A., Scott, R.P., Gregorieff, A., Bagherie-Lachidan, M., Chung, C., Lim, D.-S., et al., 2013. Yap- and Cdc42-dependent nephrogenesis and morphogenesis during mouse kidney development. PLoS Genetics 9(3): e1003380. https://doi.org/10.1371/journal.pgen.1003380.

[21] Luk, C.T., Shi, S.Y., Cai, E.P., Sivasubramaniyam, T., Krishnamurthy, M., Brunt, J.J., et al., 2017. FAK signalling controls insulin sensitivity through regulation of adipocyte survival. Nature Communications 8(1):14360. https://doi.org/10.1038/ncomms14360.

[22] Luk, C.T., Shi, S.Y., Choi, D., Cai, E.P., Schroer, S.A., Woo, M., 2013. In vivo knockdown of adipocyte erythropoietin receptor does not alter glucose or energy homeostasis. Endocrinology 154(10):3652–3659. https://doi.org/10.1210/en.2013-1113.

[23] Luk, C.T., Schroer, S.A., Woo, M., 2016. Methods for assessing the in vivo role of PTEN in glucose homeostasis. Methods in Molecular Biology 1388:75–91. Methods Mol Biol.

[24] Sinitsky, M.Y., Matveeva, V.G., Asanov, M.A., Ponasenko, A.V., 2018. Modifications in routine protocol of RNA isolation can improve quality of RNA purified from adipocytes. Analytical Biochemistry 543:128–131. https://doi.org/10.1016/j.ab.2017.12.020.

[25] Schindelin, J., Arganda-Carreras, I., Frise, E., Kaynig, V., Longair, M., Pietzsch, T., et al., 2012. Fiji: an open-source platform for biological-image analysis. Nature Methods, 676–682. https://doi.org/10.1038/nmeth.2019.

[26] Raulerson, C.K., Ko, A., Kidd, J.C., Currin, K.W., Brotman, S.M., Cannon, M.E., et al., 2019. Adipose tissue gene expression associations reveal hundreds of Candidate genes for Cardiometabolic traits. The American Journal of Human Genetics 105(4):773–787. https://doi.org/10.1016/j.ajhg.2019.09.001.

[27] Subramanian, A., Tamayo, P., Mootha, V.K., Mukherjee, S., Ebert, B.L., Gillette, M.A., et al., 2005. Gene set enrichment analysis: a knowledge-based approach for interpreting genome-wide expression profiles. Proceedings of the National Academy of Sciences of the United States of America 102(43): 15545–15550. https://doi.org/10.1073/pnas.0506580102.

[28] Mootha, V.K., Lindgren, C.M., Eriksson, K.F., Subramanian, A., Sihag, S., Lehar, J., et al., 2003. PGC-1α-responsive genes involved in oxidative phosphorylation are coordinately downregulated in human diabetes. Nature Genetics 34(3):267–273. https://doi.org/10.1038/ng1180.

[29] Stenvers, D.J., Jongejan, A., Atiqi, S., Vreijling, J.P., Limonard, E.J., Endert, E., et al., 2019. Diurnal rhythms in the white adipose tissue transcriptome are disturbed in obese individuals with type 2 diabetes compared with lean control individuals. Diabetologia 62(4):704–716. https://doi.org/10.1007/s00125-019-4813-5.

[30] Hänzelmann, S., Castelo, R., Guinney, J., 2013. GSVA: gene set variation analysis for microarray and RNA-Seq data. BMC Bioinformatics 14(1):7. https://doi.org/10.1186/1471-2105-14-7.

[31] Alsamman, S., Christenson, S.A., Yu, A., Ayad, N.M.E., Mooring, M.S., Segal, J.M., et al., 2020. Targeting acid ceramidase inhibits YAP/TAZ signaling to reduce fibrosis in mice. Science Translational Medicine 12(557):eaay8798. https://doi.org/10.1126/scitranslmed.aay8798.

[32] Shi, S.Y., Zhang, W., Luk, C.T., Sivasubramaniyam, T., Brunt, J.J., Schroer, S.A., et al., 2016. JAK2 promotes brown adipose tissue function

and is required for diet- and cold-induced thermogenesis in mice. Diabetologia 59(1):187—196. https://doi.org/10.1007/s00125-015-3786-2.

[33] Shi, S.Y., Luk, C.T., Brunt, J.J., Sivasubramaniyam, T., Lu, S.Y., Schroer, S.A., et al., 2014. Adipocyte-specific deficiency of Janus kinase (JAK) 2 in mice impairs lipolysis and increases body weight, and leads to insulin resistance with ageing. Diabetologia 57(5):1016—1026. https://doi.org/10.1007/s00125-014-3185-0.

[34] Liu, C.Y., Zha, Z.Y., Zhou, X., Zhang, H., Huang, W., Zhao, D., et al., 2010. The hippo tumor pathway promotes TAZ degradation by phosphorylating a phosphodegron and recruiting the SCFβ-TrCP E3 ligase. Journal of Biological Chemistry 285(48):37159—37169. https://doi.org/10.1074/jbc.M110.152942.

[35] Zhao, B., Li, L., Tumaneng, K., Wang, C.Y., Guan, K.L., 2010. A coordinated phosphorylation by Lats and CK1 regulates YAP stability through SCFβ-TRCP. Genes & Development 24(1):72—85. https://doi.org/10.1101/gad.1843810.

[36] Zhao, B., Wei, X., Li, W., Udan, R.S., Yang, Q., Kim, J., et al., 2007. Inactivation of YAP oncoprotein by the Hippo pathway is involved in cell contact inhibition and tissue growth control. Genes & Development 21(21):2747—2761. https://doi.org/10.1101/gad.1602907.

[37] Hansen, C.G., Ng, Y.L.D., Lam, W.L.M., Plouffe, S.W., Guan, K.L., 2015. The Hippo pathway effectors YAP and TAZ promote cell growth by modulating amino acid signaling to mTORC1. Cell Research 25(12):1299—1313. https://doi.org/10.1038/cr.2015.140.

[38] Varelas, X., 2014. The hippo pathway effectors TAZ and YAP in development, homeostasis and disease. Cambridge: Development. p. 1614—26. https://doi.org/10.1242/dev.102376.

[39] Zanconato, F., Forcato, M., Battilana, G., Azzolin, L., Quaranta, E., Bodega, B., et al., 2015. Genome-wide association between YAP/TAZ/TEAD and AP-1 at enhancers drives oncogenic growth. Nature Cell Biology 17(9):1218—1227. https://doi.org/10.1038/ncb3216.

[40] Kamura, K., Shin, J., Kiyonari, H., Abe, T., Shioi, G., Fukuhara, A., et al., 2018. Obesity in Yap transgenic mice is associated with TAZ downregulation. Biochemical and Biophysical Research Communications 505(3):951—957. https://doi.org/10.1016/j.bbrc.2018.10.037.

[41] Jing, X., Wang, J., Yin, W., Li, G., Fang, Z., Zhu, W., et al., 2018. Proliferation and differentiation of rat adipose-derived stem cells are regulated by yes-associated protein. International Journal of Molecular Medicine 42(3):1526—1536. https://doi.org/10.3892/ijmm.2018.3734.

[42] Deng, K., Ren, C., Fan, Y., Pang, J., Zhang, G., Zhang, Y., et al., 2019. YAP1 regulates PPARG and RXR alpha expression to affect the proliferation and differentiation of ovine preadipocyte. Journal of Cellular Biochemistry 120(12): 19578—19589. https://doi.org/10.1002/jcb.29265.

[43] Crewe, C., An, Y.A., Scherer, P.E., 2017. The ominous triad of adipose tissue dysfunction: inflammation, fibrosis, and impaired angiogenesis. Journal of Clinical Investigation, 74—82. https://doi.org/10.1172/JCI88883.

[44] Gregoire, F.M., Smas, C.M., Sul, H.S., 1998. Understanding adipocyte differentiation. Physiological Reviews, 783—809. https://doi.org/10.1152/physrev.1998.78.3.783.

[45] Sethi, J.K., Vidal-Puig, A.J., 2007. Thematic review series: adipocyte Biology. Adipose tissue function and plasticity orchestrate nutritional adaptation. Journal of Lipid Research 48(6):1253—1262. https://doi.org/10.1194/jlr.R700005-JLR200.

[46] Song, S., Ajani, J.A., Honjo, S., Maru, D.M., Chen, Q., Scott, A.W., et al., 2014. Hippo coactivator YAP1 upregulates SOX9 and endows esophageal Cancer cells with stem-like properties. Cancer Research 74(15):4170—4182. https://doi.org/10.1158/0008-5472.CAN-13-3569.

[47] Brodowska, K., Al-Moujahed, A., Marmalidou, A., Meyer zu Horste, M., Cichy, J., Miller, J.W., et al., 2014. The clinically used photosensitizer Verteporfin (VP) inhibits YAP-TEAD and human retinoblastoma cell growth invitro without light activation. Experimental Eye Research 124:67—73. https://doi.org/10.1016/j.exer.2014.04.011.

[48] Liu-Chittenden, Y., Huang, B., Shim, J.S., Chen, Q., Lee, S.J., Anders, R.A., et al., 2012. Genetic and pharmacological disruption of the TEAD-YAP complex suppresses the oncogenic activity of YAP. Genes & Development 26(12): 1300—1305. https://doi.org/10.1101/gad.192856.112.